Electronic Supplementary Material (ESI) for Materials Horizons.

Supplementary Information

Room-temperature synthesis of blue-emissive zero-dimensional cesium indium halide quantum dots for temperature-stable down-conversion white light-emitting diodes with a half-lifetime of 186 h

Fei Zhang, Xinzhen Ji, Wenqing Liang, Ying Li, Zhuangzhuang Ma, Meng Wang, Yue Wang, Di Wu, Xu Chen*, Dongwen Yang, Xinjian Li, Chongxin Shan and Zhifeng Shi*

Key Laboratory of Materials Physics of Ministry of Education, School of Physics and Microelectronics, Zhengzhou University, Zhengzhou 450052, China

*Corresponding author. E-mail: shizf@zzu.edu.cn; xchen@zzu.edu.cn

Table S1 Comparison of synthesis methods, morphology, size and PLQY of Cs_3InBr_6 QDs and other In-based halide materials.

Compound	Method	Morphology	Size	PLQY	Ref.
Cs_3InBr_6	M-LARP	QDs	4.5 nm	46%	**This work**
Cs_3InBr_6	Hot-injection method	Hollow NCs	20.5 nm	22.3%	[1]
$(C_6H_5CH_2NH_3)_3InBr_6$	Hydrothermal method	Single crystal	~1 cm	35%	[2]
$Cs_2InBr_5 \cdot H_2O$	Hydrothermal method	Single crystal	~2 mm	33%	[3]
$Cs_2InCl_5 \cdot H_2O$	Low temperature crystallization	Single crystal	~6 mm	18%	[4]
$Cs_2InCl_{2.5}Br_{2.5} \cdot H_2O$ $Cs_2InBr_4I \cdot H_2O$	Hydrothermal method	Single crystal	- -	24.4% 1%	[5]
$Rb_2InCl_5 \cdot (H_2O)$	Hydrothermal method	Single crystal	-	~1%	[6]
Rb_3InCl_6	Sonication method	Powder	-	-	[7]
$(C_4H_{14}N_2)_2In_2Br_{10}$	Solution-phase method	Single crystal	-	~3%	[8]

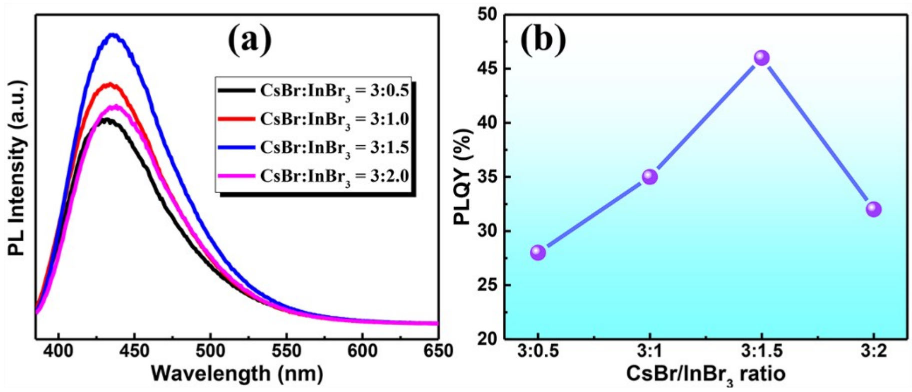

Fig. S1 (a) PL spectra and (b) PLQYs of Cs_3InBr_6 QDs synthesized under different $CsBr/InBr_3$ ratios, respectively.

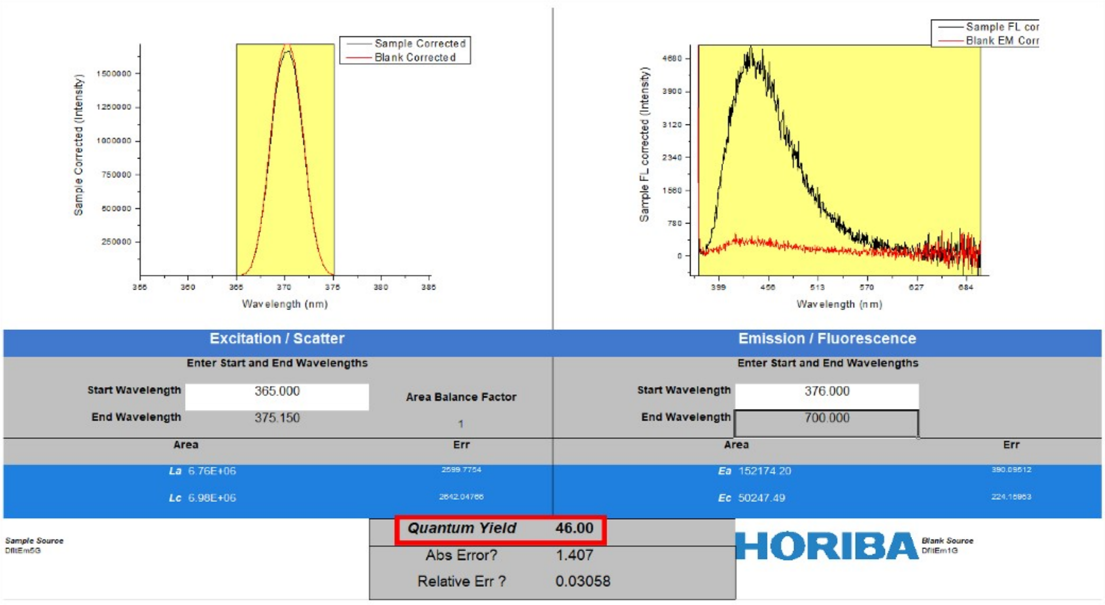

Fig. S2 PLQY data of the Cs_3InBr_6 QDs solution measured by integrating sphere.

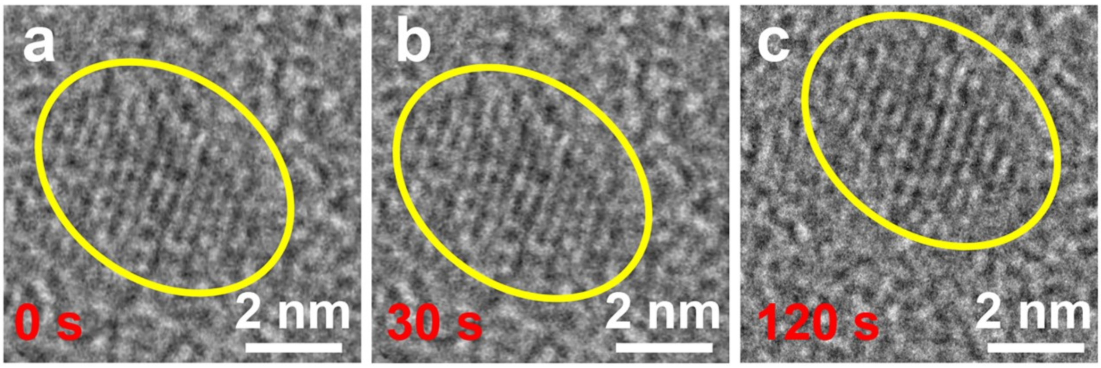

Fig. S3 TEM images of the Cs_3InBr_6 QDs continuously exposed to electron beam.

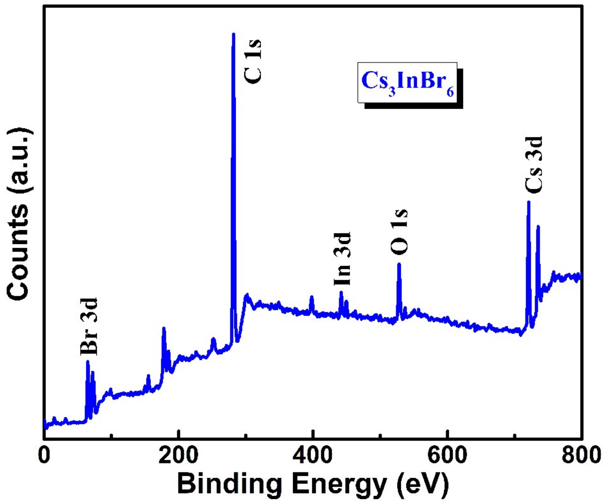

Fig. S4 Total XPS spectrum of the Cs_3InBr_6 QDs.

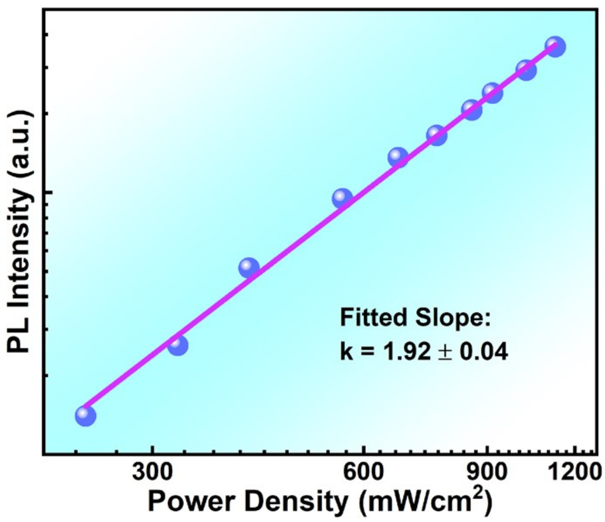

Fig. S5 Integrated PL intensity of Cs_3InBr_6 QDs as a function of excitation power density.

We further analyzed the slope of the fitted curve of the excitation-power-dependent PL emission intensity to determine the recombination kinetics. The dependence of the PL intensity I on the excitation power L can be estimated by the equation $I \approx L^k$, where k is an exponent between 0 and 2.40.[9,10] Generally, $k = 2$ indicates recombination between a free electron and a hole, $1 < k < 2$ corresponds to free or bound exciton decay, while $k < 1$ correlates with impurity-related emission. As shown in Fig. S5, the plot of log(I) *vs* log(L) is linear with a slope of 1.92 ± 0.04, indicating the exciton transition. The excitation intensity dependence of emission is consistent with the bound and free exciton emission. Considering the broadband emission feature of Cs_3InBr_6 QDs, the PL emission in Cs_3InBr_6 is essentially excitonic and results from the recombination of bound excitons and multiphonon emission.

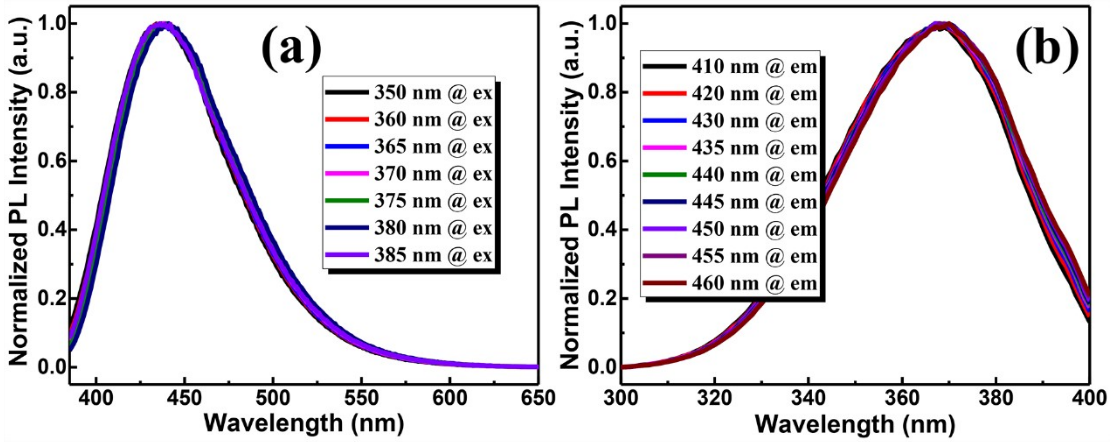

Fig. S6 (a) Normalized PL spectra of Cs_3InBr_6 QDs monitored at different excitation wavelengths. (b) Normalized PL excitation spectra of Cs_3InBr_6 QDs monitored at different emission wavelengths.

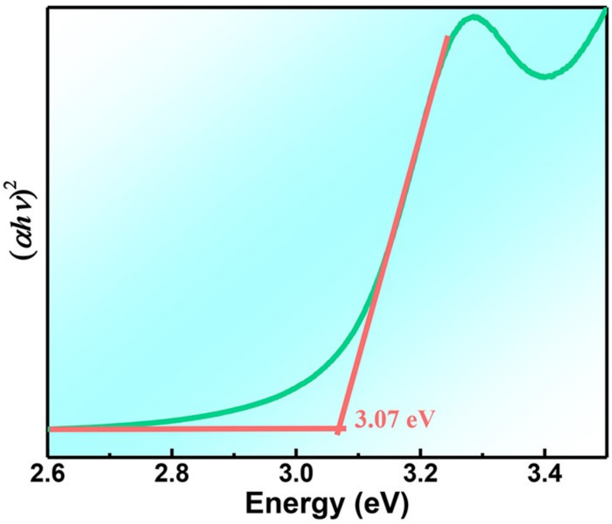

Fig. S7 The bandgap of Cs_3InBr_6 QDs determined from a Tauc plot of absorption spectrum.

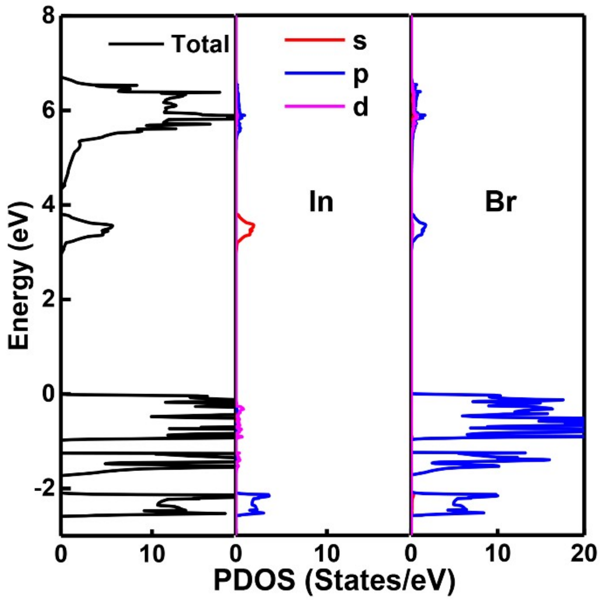

Fig. S8 The predicted density of states (PDOS) of Cs_3InBr_6 using PBE functional.

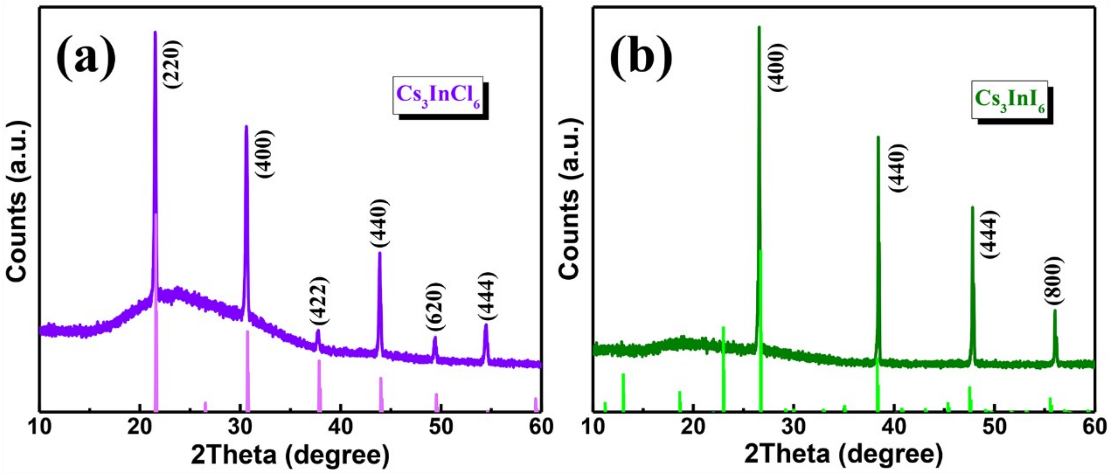

Fig. S9 XRD patterns of (a) Cs_3InCl_6, and (b) Cs_3InI_6 QDs, respectively.

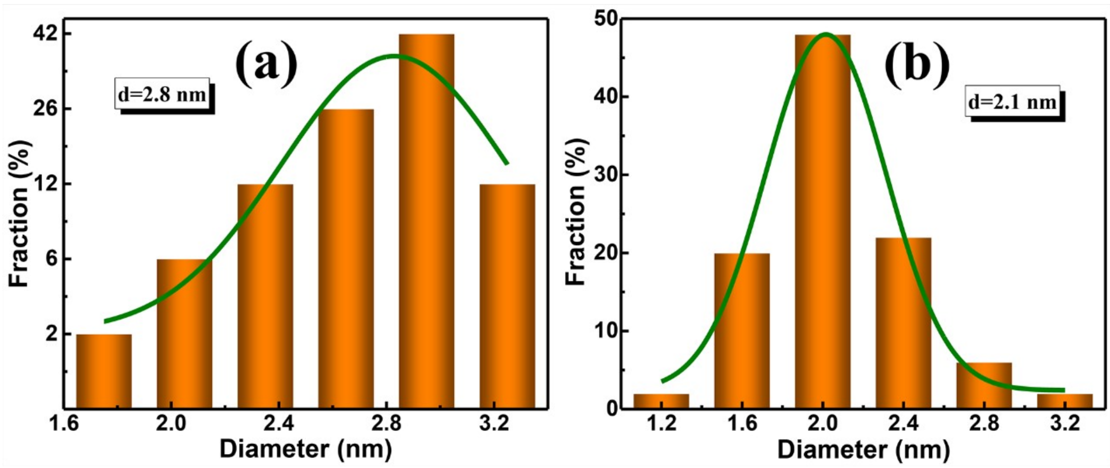

Fig. S10 Size distribution histograms of (a) Cs_3InCl_6, and (b) Cs_3InI_6 QDs, respectively.

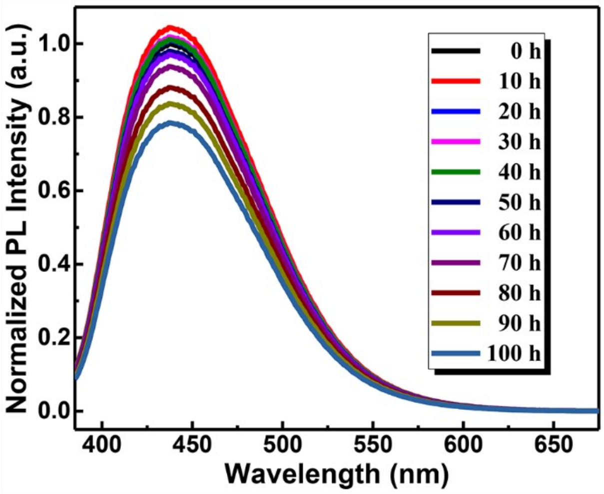

Fig. S11 PL spectra evolution of the Cs_3InBr_6 QDs under different UV light irradiation time.

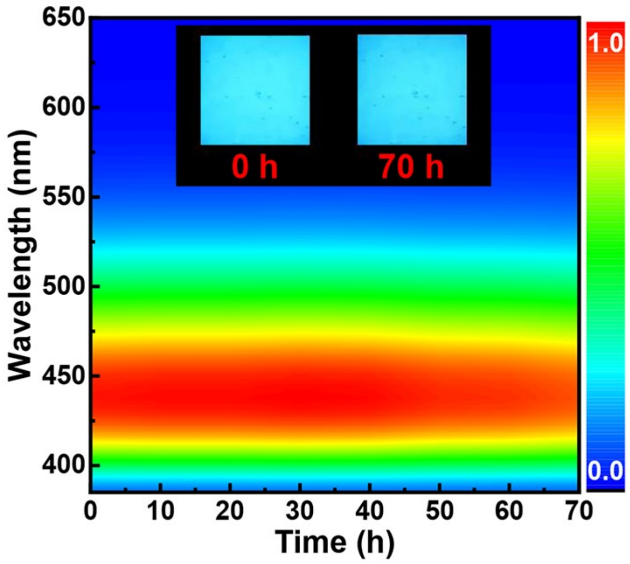

Fig. S12 Stability test of the Cs_3InBr_6 QDs film under continuous 365 nm UV lamp irradiation and high humidity (20−30 °C, 70−80% humidity) environment. The insets show the luminescence photos of the Cs_3InBr_6 QDs film before and after treatment.

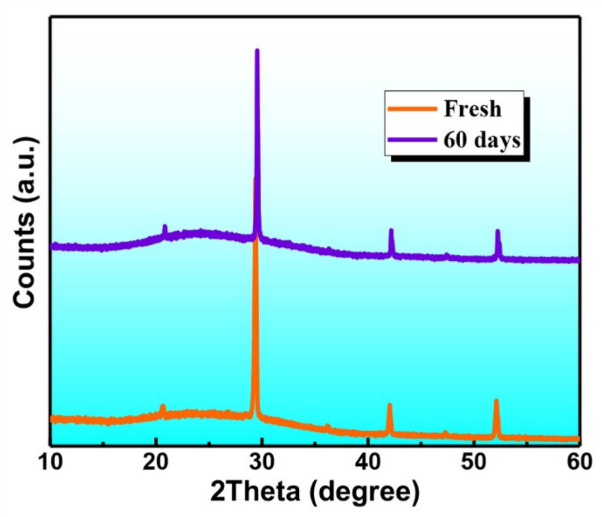

Fig. S13 XRD results of the Cs_3InBr_6 QDs film after storage in air ambient (20−35 °C, 50−60% humidity) for 60 days.

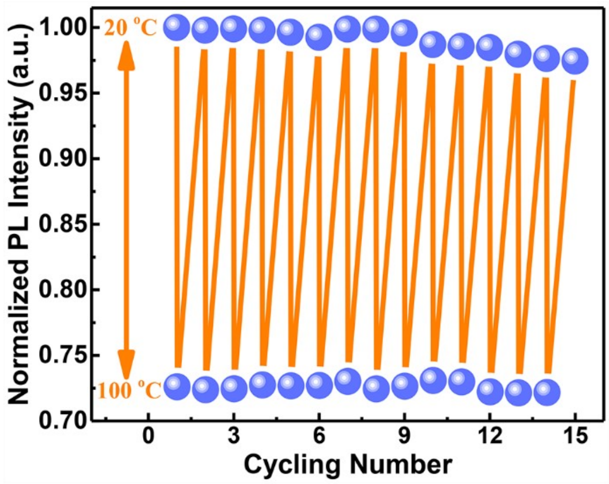

Fig. S14 Plots of the normalized PL intensity of Cs_3InBr_6 QDs at two typical temperature points (20 °C and 100 °C) over 15 heating/cooling cycles.

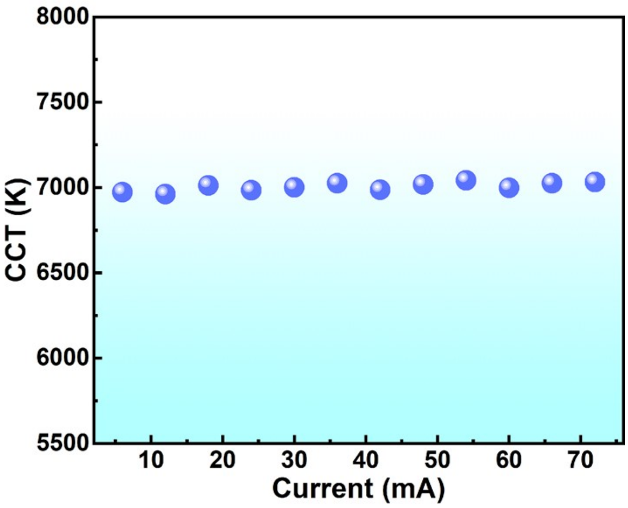

Fig. S15 The corresponding color temperature (CCT) of the WLED under different driving currents.

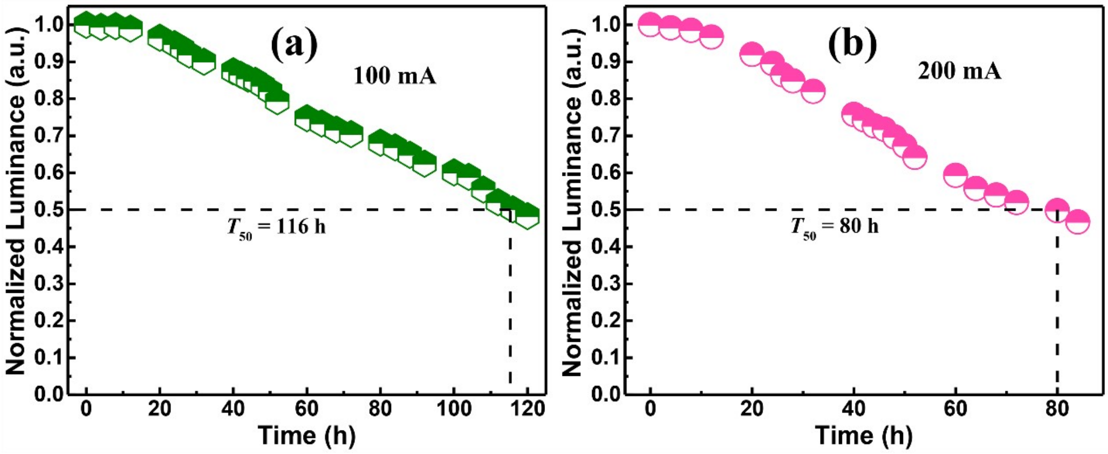

Fig. S16 Emission intensity evolution of the WLED measured at the driving current of (a) 100 mA, and (b) 200 mA, respectively.

References

[1] F. Zhang, D. Yang, Z. Shi, C. Qin, M. Cui, Z. Ma, L. Wang, M. Wang, X. Ji, X. Chen, D. Wu, X. Li, L. Zhang and C. Shan, *Nano Today,* 2021, **38**, 101153.

[2] D. Chen, S. Hao, G. Zhou, C. Deng, Q. Liu, S. Ma, C. Wolverton, J. Zhao and Z. Xia, *Inorg. Chem.,* 2019, **58**, 15602.

[3] L. Zhou, J. F. Liao, Z. G. Huang, J. H. Wei, X. D. Wang, W. G. Li, H. Y. Chen, D. B. Kuang and C. Y. Su, *Angew. Chem. Int. Ed.,* 2019, **58**, 5277.

[4] X. Liu, X. Xu, B. Li, Y. Liang, A. Li, H. Jiang and D. Xu, *CCS Chem.,* 2020, **2**, 216.

[5] Y. Jing, Y. Liu, X. Jiang, M. S. Molokeev, Z. Lin and Z. Xia, *Chem. Mater.,* 2020, **32**, 5327.

[6] P. Han, C. Luo, S. Yang, Y. Yang, W. Deng and K. Han, *Angew. Chem. Int. Ed.,* 2020, **59**, 12709.

[7] J. D. Majher, M. B. Gray, T. Liu, N. P. Holzapfel and P. M. Woodward, *Inorg. Chem.,* 2020, **59**, 14478.

[8] L. Zhou, J. F. Liao, Z. G. Huang, J. H. Wei, X. D. Wang, H. Y. Chen and D. B. Kuang, *Angew. Chem. Int. Ed.,* 2019, **58**, 15435.

[9] T. Schmidt, K. Lischka and W. Zulehner, *Phys. Rev. B*, 1992, **45**, 8989.

[10] X. Li, X. Lian, J. Pang, B. Luo, Y. Xiao, M. D. Li, X. C. Huang and J. Z. Zhang, *J. Phys. Chem. Lett.*, 2020, **11**, 8157.